Accelerated Electrons in Cassiopeia A: An Explanation for the Hard X-Ray Tail

J. Martin Laming

E. O. Hulburt Center for Space Research, Naval Research Laboratory, Code 7674L, Washington DC 20375

jlaming@ssd5.nrl.navy.mil

ABSTRACT

We propose a model for the hard X-ray (> 10 keV) emission observed from the supernova remnant Cas A. Lower hybrid waves are generated in strong (mG) magnetic fields, generally believed to reside in this remnant, by shocks reflected from density inhomogeneities. These then accelerate electrons to energies of several tens of keV. Around 4% of the x-ray emitting plasma electrons need to be in this accelerated distribution, which extends up to electron velocities of order the electron Alfvén speed, and is directed along magnetic field lines. Bremsstrahlung from these electrons produces the observed hard x-ray emission. Such waves and accelerated electrons have been observed in situ at Comet Halley, and we discuss the viability of the extrapolation from this case to the parameters relevant to Cas A.

Subject headings: acceleration of particles—radiation mechanisms: non-thermal—shock waves—supernova remnants

1. Introduction

A number of supernova remnants have recently been recognized as likely acceleration sites for cosmic ray electrons. SN 1006 (Koyama et al. 1995) and G347.3-0.5 (Slane et al. 1999; Koyama et al. 1997) both show spectra with continua so strong in the spectral region around 1 keV that no line emission is detectable with e.g. the Advanced Satellite for Cosmology and Astrophysics (ASCA). Laming (1998) has shown for SN 1006 that any explanation based on non-thermal bremsstrahlung fails. It must either produce line emission that should be observable, or in the most extreme case of a shock propagating through a pure carbon plasma (which will produce no lines in the bandpass of instruments such as ASCA), the amount of carbon required to produce the observed intensity is well in excess of that expected for a Type Ia supernova, and indeed exceeds the Chandrasekhar limit by large factors. Thus synchrotron radiation from cosmic ray electrons with energies of order 100 TeV is left as the only viable interpretation. This conclusion is essentially confirmed by the detection of TeV γ -rays from SN 1006 by Tanimori et al. (1998).

A second class of cosmic ray accelerator candidates do show the line emission expected, but also have a hard X-ray "tail" to their X-ray spectra. Members of this class include Cas A (Allen et al. 1997; Favata et al. 1997), IC 443 (Keohane et al. 1997), and possibly RCW 86 (Allen et al. 1998). While less compelling than the first class, no other mechanism has been postulated to date that could explain the approximate power law behaviour of the emission, seen in Cas A up to energies in excess of 100 keV (Allen et al. 1997; The et al. 1996). It is the purpose of this paper to investigate such a possibility, where collective motions of the plasma (specifically lower hybrid waves) excited by ions reflected from shock front decay accelerating electrons into a non-Maxwellian distribution function. We begin by reviewing the simplest models for collisionless shocks. Section 2 reviews the theory of electron energization by lower hybrid waves, which has received recent attention in connection with cometary X-ray emission (Bingham et al. 1997; Shapiro et al. 1999). Section 3 describes the application of these results to Cas A, while section 4 discusses the assumptions underlying this approach, and some of the consequences for our understanding of Cas A that such a model, if correct, would yield.

Assuming that the gas pressure >> magnetic pressure in the downstream plasma, the temperature T_a reached by particle species a with mass m_a is given by conservation of energy, momentum and particles across the shock discontinuity by

$$k_B T_a = \frac{3}{16} m_a v_s^2 \tag{1}$$

for shock velocity v_s . Thus in the limit of true collisionless plasma, the particles will have temperature proportional to their masses, i.e. protons will have a temperature $m_i/m_e = 1836$ times that of the electrons. Obviously in realistic conditions Coulomb equilibration will take place, with rate

$$\frac{d\Delta T}{dn_e t} = -0.13 \frac{Z}{A} \frac{\Delta T}{T_e^{3/2}} \tag{2}$$

in c.g.s. units, where $\Delta T = T_i - T_e$, and the ions have charge Z and atomic mass A. So long as $T_i >> T_e$ we can integrate to get

$$T_e = \left(\frac{5}{2} \times 0.13 \frac{Z}{A} T_i n_e t\right)^{2/5}.$$
(3)

Averaging this temperature over the life of the shock modifies T_e by an extra factor 5/7. Such a model, assuming values of Z in the range 8-26 (corresponding to oxygen and its burning products) adequately explains the observed temperatures of shocked ejecta and circumstellar medium (CSM), 1.25 and 3.8 keV respectively for $n_eT \sim 10^{11}$ cm⁻³s in each case in Cas A (Favata et al. 1997), but cannot explain the hard x-ray continuum extending out to 100 keV.

2. The Electron Distribution Function from Lower Hybrid Wave Damping

From observations of radio synchrotron emission Cas A is believed to have relatively high magnetic fields, perhaps up to the equipartition value of order 1 mG (Gull 1975; Keohane, Gotthelf,

& Petre 1998). A total energy in cosmic ray electrons and magnetic field of ~ 10^{49} erg is required (c.f. Longair 1994), which for maximum synchrotron luminosity must be equipartitioned between the two. If distributed uniformly throughout the Cas A shell, this evaluates to a magnetic field of 0.5 mG. Thus lower hybrid waves excited by cross field ion motions can accelerate electrons into a high energy tail onto the otherwise thermal Maxwellian distribution function. These are electrostatic ion waves that occur when the electrons are magnetized, which is likely to be the case at so-called quasi-perpendicular shocks. Due to the the shock compression of the magnetic field component perpendicular to the shock velocity vector, quasi-perpendicular shocks are likely to be more prevalent than quasi-parallel shocks in Cas A, and in supernova remnants in general, and will be assumed throughout this paper. Electron velocities at least up to the electron Alfvén velocity, $B/\sqrt{4\pi n_e m_e}$ where B is the magnetic field strength, and n_e and m_e are the electron density and mass respectively, are possible. This corresponds to energies of order 100 keV for Cas A, making it an attractive mechanism to explore.

Electrons accelerated by these waves emit bremsstrahlung radiation, and have been recently discussed as a mechanism for cometary x-ray emission. Neutral atoms or molecules outgassing from a comet nucleus can be photoionized by solar UV radiation. In the interaction of these stationary (in the comet rest frame) ions with the ambient solar wind, a modified two-stream instability develops that in the case of magnetic field perpendicular to the relative comet-solar wind velocity generates lower hybrid waves (Bingham et al. 1997; Shapiro et al. 1999).

We will apply a similar model to Cas A, following in part the analytic treatments of Vaisberg et al. (1983), Krasnosel'skikh et al. (1985), and Begelman & Chiueh (1988), where ions reflected from shock fronts in Cas A move back upstream through the preshock plasma generating a similar modified two-stream instability. Such reflected ions and associated wave generation are common features in in situ observations of solar system shocks (c.f. Lengyel-Frey et al. 1997), and of models of electron energization at collisionless shocks (c.f. Cargill & Papadopoulos 1988; Tokar et al. 1986; McClements et al. 1997; Vaisberg et al. 1983; Krasnosel'skikh et al. 1985). Vaisberg et al. (1983) give an analytic form for the electron distribution function following lower hybrid wave energization, which agrees well with the particle-in-cell simulations performed by Shapiro et al. (1999). The mathematical development of the theory for these waves is summarized in Appendix A. It is shown that for both reactive and kinetic forms of the instability, wave growth is strongest for wavevectors with a small parallel component $k_{\parallel}/k \leq \omega_{pi}/\omega_{pe}$. Hence the wave can simultaneously be in resonance with ions moving across and electrons moving parallel to the magnetic field, since the phase velocities are much larger along the magnetic field than across it. This facilitates energy transfer between electrons and ions. The resulting electron distribution function parallel to the magnetic field is also derived in Appendix A.

However the wave group velocity away from the shock front is lower than the shock velocity itself for $k_{||}/k < \omega_{pi}/\omega_{pe}$. Only at $k_{||}/k = \omega_{pi}/\omega_{pe}$ or greater can the waves stay ahead of the shock. This is important because the growth rates, particularly for the kinetic form of the instability, are not large, and for smaller $k_{||}$ the waves are likely to be overrun by the shock before significant

growth can occur. Hence in the following we assume that in the preshock region, a significant level of wave activity exists only for $k_{||}/k = \omega_{pi}/\omega_{pe}$. With this simplification the accelerated electron distribution function is then given by equation (A17) with $\cos \theta = \omega_{pi}/\omega_{pe}$

$$f_e(v_{||}) = \frac{n'_i}{\sqrt{2\pi}k_B T/m_i} \exp\left(-\frac{1}{2}\right) \frac{\omega_{pi}^2}{\omega_{pe}^2} \left(v_m - v_{||} + \frac{\left(v_m^3 - v_{||}^3\right)}{3v_{Ae}^2}\right)$$
(4)

where $v_{Ae} = v_{Ai}\sqrt{m_i n_i/m_e n_e}$ is the electron Alfvén velocity, $(v_{Ai} = B/\sqrt{4\pi n_i m_i})$ being the usual Alfvén velocity), n'_i is the density of shock reflected ions, and v_m is a constant of integration, denoting the maximum electron velocity. In the quasi-linear theory used in Appendix A, the accelerated electron density, n'_e , or v_m remains a single free parameter. They are related by

$$n'_{e} = \frac{n'_{i}}{\sqrt{2\pi}k_{B}T/m_{i}} \exp\left(-\frac{1}{2}\right) \frac{\omega_{pi}^{2}}{\omega_{pe}^{2}} \left(v_{m}^{2} + \frac{v_{m}^{4}}{2v_{Ae}^{2}}\right).$$
(5)

where an extra factor of two has been included to include the electron velocity range $-v_m \rightarrow +v_m$.

For a reflected ion population $\sim 25\%$ of the preshock ion density (c.f. Cargill & Papadopoulos 1988; McClements et al. 1997, and references therein), we get

$$\frac{n'_e}{n_e} = 0.06 \left(\frac{v_m^2}{v_{Ae}^2} + \frac{v_m^4}{2v_{Ae}^4} \right) \frac{m_e}{m_i} \frac{v_{Ae}^2}{v_{ti}^2}.$$
(6)

Anticipating from the following section that $n'_e/n_e \simeq 4\%$, $v_{Ae} \sim 26v_s$ and $v_{ti} = 0.53v_s$ (assuming complete equipartition of magnetic and ion thermal energy, but insignificant electron-ion equilibration) gives $v_m = v_{Ae}\sqrt{\sqrt{1+A}-1}$ where A is the atomic mass of the ions. Hence $v_m \sim v_{Ae}$, slowly increasing with the ion mass.

3. Application to Cassiopeia A

We compute model bremsstrahlung spectra using the distribution function given by equation (4) above for the electron velocity parallel to the magnetic field, representing the electron velocity perpendicular to the magnetic field as Maxwellians. The temperature for these perpendicular components is taken to be the same as that fitted to the thermal bremsstrahlung emitted at energies less than 10 keV. A fit to the BeppoSAX Medium Energy Concentrator (MECS Boella et al. 1997) spectrum from 1997 November 26 determined this temperature at 3.3 keV. This fit is shown in Figure 1. Other workers find temperatures in the range 2.9-4.2 keV (Allen et al. 1997; Favata et al. 1997; Vink, Kaastra, & Bleeker 1996) from ASCA and BeppoSAX data.

The non-relativistic bremsstrahlung cross section $d\sigma$ for photon emission with energy in the range $E \rightarrow E + dE$ is given by (Berestetskii, Lifshitz, & Pitaevskii 1982)

$$d\sigma = -\frac{d}{dz} \left| {}_{2}F_{1}\left(\frac{iZ}{v_{f}}, \frac{iZ}{v_{i}}, 1, z\right) \right|^{2} \frac{64\pi^{2}}{3} Z^{2} \alpha r_{0}^{2} \frac{m_{e}^{2}c^{2}}{\left(p_{i} - p_{f}\right)^{2}} \frac{p_{f}}{p_{i}} \frac{1}{\left(1 - \exp\left(-2\pi Z/v_{f}\right)\right) \left(\exp\left(2\pi Z/v_{i}\right) - 1\right)} \frac{dE}{E} \frac{dE}{dz} \left(\frac{iZ}{v_{f}}, \frac{iZ}{v_{i}}, 1, z\right) \right|^{2} \frac{64\pi^{2}}{3} Z^{2} \alpha r_{0}^{2} \frac{m_{e}^{2}c^{2}}{\left(p_{i} - p_{f}\right)^{2}} \frac{p_{f}}{p_{i}} \frac{1}{\left(1 - \exp\left(-2\pi Z/v_{f}\right)\right) \left(\exp\left(2\pi Z/v_{i}\right) - 1\right)} \frac{dE}{E} \frac{iZ}{v_{f}} \left(\frac{iZ}{v_{f}}, \frac{iZ}{v_{i}}, 1, z\right) \right)^{2} \frac{64\pi^{2}}{3} Z^{2} \alpha r_{0}^{2} \frac{m_{e}^{2}c^{2}}{\left(p_{i} - p_{f}\right)^{2}} \frac{p_{f}}{p_{i}} \frac{1}{\left(1 - \exp\left(-2\pi Z/v_{f}\right)\right) \left(\exp\left(2\pi Z/v_{i}\right) - 1\right)} \frac{dE}{E} \frac{iZ}{v_{f}} \left(\frac{iZ}{v_{f}}, \frac{iZ}{v_{i}}, 1, z\right) \left(\frac{iZ}{v_{f}}, \frac{iZ}{v_{i}}, \frac{iZ}$$

where p_i , p_f , v_i , v_f are initial and final electron momenta and velocities, Z is the nuclear charge, α is the fine structure constant, and r_0 is the classical electron radius. Using standard formulae for manipulating the hypergeometric function ${}_2F_1$ and its derivative in the limit of low Z/v_i and Z/v_f a simpler form suitable for evaluation of the double integral to compute the emission rates can be found;

$$d\sigma = \frac{64\pi^2}{3} Z^2 \alpha r_0^2 \frac{c^2}{v_i^2} \frac{Z/v_f}{(1 - \exp\left(-2\pi Z/v_f\right))} \frac{Z/v_i}{(\exp\left(2\pi Z/v_i\right) - 1)} \log\left(\frac{p_i + p_f}{p_i - p_f}\right) \frac{dE}{E}.$$
 (8)

In checks against bremsstrahlung spectra computed with the full formula given by equation (7) (Sutherland 1998), the simpler equation (8) was found agree at the few percent level for Maxwellian electron distributions, for temperatures appropriate to Cas A for target charges up to 8 (i.e. a fully ionized oxygen plasma). Cas A has very little hydrogen. Oxygen is probably the most abundant element (Vink, Kaastra, & Bleeker 1996).

In Figures 2 and 3 we plot spectra from the BeppoSAX MECS and the higher photon energy Phoswich Detector System (PDS Frontera et al. 1997) instruments, together with model spectra. The softest model spectrum in Figure 2 is a pure thermal bremsstrahlung spectra at 3.3 keV in fully ionized oxygen. The emission measure for this spectrum is $n_e n_O V = 3.05 \times 10^{57}$ cm⁻³ for an assumed distance to Cas A of 3.4 kpc (Reed et al. 1995). The successively harder spectra have been computed by taking 4% of these thermal electrons and putting them into a lower hybrid wave energized distribution function, for electron Alfvén velocities of 32, 40, and 48 atomic units (in atomic units, $e = \hbar = m_e = 1$, so the atomic unit of velocity is 2.188×10^8 cm s⁻¹), with $v_m = 1.77v_{Ae}$. Figure 3 shows the same data with the pure thermal bremsstrahlung and nonthermal bremsstrahlung models for v_{Ae} of 56, 68, and 80 atomic units for a pure He plasma, with $v_m = 1.11v_{Ae}$. In both cases, the curves with $v_m \sim 70$ atomic units appear to give the best match to the data up to energies ~ 50 keV.

4. Discussion

4.1. The Morphology of Cas A

One immediate problem is that the mG magnetic fields are present only inside the Cas A remnant (presumably amplified by Rayleigh-Taylor instabilities at the contact discontinuity), whereas most shock models require such fields to be present *ahead* of the shock (to be discussed in more detail below). However Cas A is an extremely inhomogeneous supernova remnant. It has numerous knots of optical emission from low charge states, which must be considerably denser than the surrounding plasma so that the recombination and radiative cooling times are sufficiently short. The blast wave travelling through the circumstellar material will to split into transmitted and reflected shocks upon meeting these inhomogeneities (see Sgro 1975; Borkowski, Blondin, & Sarazin 1992, for fuller discussion). Indeed exactly this happens in the simulations of Borkowski et al. (1996), giving rise to the possibility that shock waves are propagating throughout the X-ray and radio emitting shell. Since the plasma has already been heated by the blast wave or reverse shock these shocks will most likely be of relatively low Mach number (but still supercritical; see subsection 4.5 below). Another possibility for inhomogeneous or clumpy SNR is that the Rayleigh-Taylor fingers from the unstable contact discontinuity can propagate outwards and penetrate through the forward shock (Jun, Jones, & Norman 1996). The by-now famous Chandra x-ray images (Hwang, Holt, & Petre 2000) suggest that both scenarios could indeed be true. The forward shock is visible as a faint ring around the outside of the bright x-ray shell, which has its origin in shocked ejecta. The boundary between faint and bright emission is the contact discontinuity, which has no obvious penetration through the blast wave, except in the "jet" region in the NE quadrant. However the apparent "inversion" of the presumed pre-supernova element stratification (Hughes et al. 2000; Hwang, Holt, & Petre 2000), with Fe being found in outer regions of the eastern part of the remnant with respect to lighter elements like Si, suggests a role for the Raleigh-Taylor instability, and makes it more likely that these regions have come into contact with strong magnetic fields at the contact discontinuity. Lower hybrid electron acceleration is also more likely in the heaviest element plasmas, (i.e. the Fe ejecta), for reasons discussed in the next subsection.

4.2. The Thermal Electron Temperature

The lifetime of accelerated electrons against Coulomb collisions with the thermal background is $t \simeq 5 \times 10^6 (E/1 \text{ keV})^{3/2}$ s which evaluates to 14 - 150 years for electron energies of 20 - 100 keV. Hence electron acceleration must be ongoing, or have ceased in the very recent past, though this last possibility seems unlikely since the hard x-ray emission from Cas A has been known since the earliest days of x-ray astronomy (Gorenstein, Kellogg, & Gursky 1970).

In section A.4 of the Appendix it is shown that an appropriate criterion for the presence of lower hybrid waves is that the electron gyroradius should be less than the wavelength, which can be expressed as $T_e/T_i < \Omega_e^2/Z/\omega_{pe}^2$. In a magnetic field of 1 mG and electron density of 10 cm⁻³ this evaluates to $T_e << 3 \times 10^6 (v_s/4000 \text{km s}^{-1})^2$. The shock velocity has been determined from proper motion studies. For the same assumed distance as before, radio data give an expansion velocity of ~ 2000 km s⁻¹ (Anderson & Rudnick 1995), while X-ray studies give velocities of ~ 3500 km s⁻¹ for the bright ring at a radius of 110", and ~ 5200 km s⁻¹ inferred for the blast wave at a radius of 160" (Vink et al. 1998), all of which require T_e significantly lower than that observed. As discussed in section A.4, an alternative condition on the electron Landau damping rate requires $k_BT << m_e \Omega_{LH}^2/k_{||}^2$, which is the same as above for $k_{||}/k \simeq \omega_{pi}/\omega_{pe}$, but less restrictive for smaller $k_{||}$. The first criterion is also not met in the plasma around the nucleus of Comet Halley where lower hybrid waves and accelerated electrons were directly detected in situ (Gringauz et al. 1986; Klimov et al. 1986). They observed $\Omega_{LH} \sim 100$ rad s⁻¹, and $n_e \simeq 300$ cm⁻³ giving $\Omega_e^2/\omega_{pe}^2 \sim 2 \times 10^{-5}$, while $T_e \sim 2 \times 10^5$ K and $T_i \sim 10^7$ K.

One plausible solution to this dilemma is that in the region of wave generation, the electron

temperature is in fact lower than the estimates and observations above would indicate. This is possible if the electrons are not energized on passage through the shock due to being bound to ions, only becoming ionized some time later on either by collisions in Cas A or by photoionization in Comet Halley. This is demonstrated in calculations of the Cas A reverse shock propagating through clumps of Fe ejecta by Mochizuki et al. (1999), where temperatures satisfying the condition on the electron gyroradius are found. Thus for Cas A the hard x-ray emission is more likely to be associated with regions of shocked ejecta where many electrons are still being ionized from bound states. In order that this putative ionizing region in Cas A should produce enough bremsstrahlung emission to be visible against the thermal continuum, a higher background ion charge might be necessary. This is also more likely if the thermal bremsstrahlung continuum with $T_e = 4 \times 10^7$ K comes from the shocked circumstellar medium, composed of He, N, and possibly O, while the non-thermal component comes from the ejecta, composed of O and heavier elements. Thus the local fraction of accelerated electrons may be different from the 4% determined above by matching to the BeppoSAX MECS/PDS spectra. However the maximum accelerated electron velocity $v_m \propto (n'_e/n_e)^{1/4}$ is relatively insensitive to this, making large changes in the bremsstrahlung spectrum from that calculated before unlikely. The temperature assumed above for the perpendicular components of the accelerated electron distribution will also change. Again this will not significantly alter the non-thermal bremsstrahlung spectrum.

Another reason for spatially separating the thermal and non-thermal bremsstrahlung emitting regions is that over the 300 years or so of the remnant's existence, collisions between the accelerated and thermal electrons would be likely to have raised the thermal electron temperature to a value well in excess of that observed if they were cospatial.

4.3. The Electron Alfvén Speed

Another crucial parameter in determining the visibility of non-thermal bremsstrahlung is the electron Alfvén velocity. From observations of radio synchrotron emission, Cas A is believed to have a large magnetic field ~ 1 mG, generated by turbulence associated with Rayleigh-Taylor instabilities at the contact discontinuity between the shocked ejecta and circumstellar material (c.f Gull 1975; Keohane, Gotthelf, & Petre 1998). Assuming such instabilities generate magnetic fields up to equipartition, we may write

$$\frac{B^2}{8\pi} = \frac{1}{2} \left(n_i k_B T_i + n_e k_B T_e \right) \tag{9}$$

where T_i and T_e are given by the shock jump conditions (equation 1). The resulting electron Alfvén velocity thus becomes

$$v_{Ae} = \sqrt{\frac{B^2}{4\pi n_e m_e}} = v_s \sqrt{\frac{3m_p}{8m_e}} = 26v_s \tag{10}$$

for fully ionized plasmas where nuclear mass Am_p is such that A = 2Z. The X-ray blast wave velocity (discussed above) gives $v_{Ae} \simeq 60$ atomic units according to equation (10), with correspondingly lower values from the other observations. This is more than adequate to give a sufficiently high v_{Ae} for the non-thermal bremsstrahlung to originate in oxygen or heavier element plasma. Hard x-rays from a helium plasma require higher v_{Ae} , still consistent with the observed x-ray blast wave, but not with the lower inferred shock velocities.

4.4. High Energy Behaviour of the Continuum and ⁴⁴Ti

The highest energy data points (above 100 keV) may still possibly require the existence of cosmic rays. As can be seen in Figures 2 and 3, v_{Ae} or v_m cannot be arbitrarily increased to reproduce this emission without overestimating the non-thermal continuum at lower energies. However in principle relativistic electron energies are possible from lower hybrid wave acceleration (Mc-Clements et al. 1997; Vaisberg et al. 1983). The maximum cutoff in our approach stems from taking only waves with $k_{\parallel}/k = \omega_{pi}/\omega_{pe}$, which satisfies the requirement that the perpendicular group velocity of the waves be greater than the shock velocity, to allow sufficient time for wave growth. With stronger reactive instabilities, waves with $k_{\parallel} \rightarrow 0$ may exist at sufficient intensity to make electron acceleration by lower-hybrid waves a plausible mechanism for solving the so-called electron injection problem (McClements et al. 1997). This arises because first order Fermi acceleration at quasi-perpendicular shock fronts is only effective for electrons of mildly relativistic or higher energies (Levinson 1996), and so some other "injection" mechanism is required.

The question of the spectral behaviour at high energies is further confused slightly by the discrepancy in fluxes observed above 100 keV by BeppoSAX and OSSE. Compared with the data from OSSE presented in Figure 2 of Allen et al. (1997), the BeppoSAX PDS fluxes are up to an order of magnitude higher above 100 keV. Cas A is unlikely to be a variable source at these (or any other) energies, and so this problem presumably lies with the calibration of one or other of the instruments.

Another issue complicating the comparison of continuum spectra, but of supreme interest in its own right, is the possibility of detecting γ -ray line emission from the nucleus ⁴⁴Sc at energies of 67.9 and 78.4 keV. ⁴⁴Sc is a decay product of ⁴⁴Ti, which is one of the most important radioactive elements produced in the α -rich freeze out of core collapse supernovae, its abundance also being sensitive to the position of the mass cut (c.f Vink et al. 2000, for further discussion). The break in the lower-hybrid wave accelerated electron spectrum occurs at energies very close to where the ⁴⁴Sc lines should be present, and the substitution of the power law in the fit to the BeppoSAX PDS data by Vink et al. (2000) with the non-thermal bremsstrahlung spectrum modeled in this paper might lead to interesting results for the flux in these lines.

4.5. Properties of Collisionless Shocks

So far we have invoked the excitation of lower hybrid waves ahead of a shock front, and modeled the electron distribution function on the assumption that a quasi-steady state can be reached in the shock rest frame. We will discuss these assumptions in more detail here.

In a number of models, various types of plasma waves are excited by ions that are reflected from the shock front and travel back upstream. This generally arises in perpendicular shocks due to the cross shock ambipolar electric field in the magnetic field overshoot region. The simulation of Cargill & Papadopoulos (1988) has reflected ions exciting electron plasma waves and then ion acoustic waves to provide eventual electron heating to around 20% of the postshock ion temperature. McClements et al. (1997) looked at the excitation of lower hybrid waves by ion gyrating in the magnetic field upstream of a fast shock, with a view to modeling the injection mechanism for the Fermi acceleration of electrons to cosmic ray energies at perpendicular shocks. A certain amount of support for these models comes from observations of shock waves in the solar wind where electron plasma and ion acoustic waves are seen ahead of shock fronts (Lengyel-Frey et al. 1997), and lower hybrid waves (Klimov et al. 1986) and their associated electron distribution function (Gringauz et al. 1986) have also been observed at comet Halley, with Shapiro et al. (1999) recently demonstrating by particle-in-cell simulations that the observed wave activity is indeed consistent with the observed electron distribution function.

An important point concerns the nature of the two-stream instability. All of the models discussed above assume the ions reflected from the shock to be essentially monoenergetic, thus giving rise to fast growing reactive instabilities. At perpendicular shocks this is necessary since the reflected ions only move back upstream for about an ion gyroradius before begin swept back behind the shock front, thus allowing only a finite amount of time for the instability to develop. This monoenergetic property of the reflected ions surprisingly appears to persist in shock simulations to high Mach numbers, where the shocks themselves should be highly turbulent (Cargill & Papadopoulos 1988; Tokar et al. 1986). Both sets of authors comment that the ion reflection in their simulations becomes "bursty", giving a time average of $\sim 25\%$; not too different from the fraction of preshock ions observed to be reflected at lower Mach number (less turbulent) shocks in the solar wind or laboratory experiments. Woods (1987) emphasises that such ion reflection is characteristic of a very thin shock transition. For thicker shocks, the ions will gyrate in the magnetic field before reflection to varying degrees, giving rise to a reflected ion distribution still monoenergetic, but having a finite angular spread. Woods (1987) terms this a transition from "specular" to "diffuse" reflection. Gedalin (1996) has considered this distinction in more quantitative detail. Diffusely reflected ions will produce slower growing instabilities ahead of the shock, and hence produce less electron heating, and have been suggested as a possible reason by Laming (1998) for the low amount of collisionless electron heating observed at fast ($\sim 2600 \text{ km s}^{-1}$) shocks in the NW region of SN 1006 by Laming et al. (1996).

We have argued above that based on our knowledge of the properties of Cas A, the shocks

producing the reflected ions and lower hybrid waves are likely to be of relatively low Mach number, since they are reflected from density inhomogeneities and are propagating through plasma that has already been heated by the forward or reverse shocks. Hence a "bursty" ion reflection is unlikely, and the assumption of steady state conditions embodied in equation (A15) remains valid. The sound speed in plasma shocked by the blast wave with speed v_s and with no electron-ion equilibration is $\sqrt{5k_BT_i/3m_i} = \sqrt{5/16}v_s$. This plasma continues expanding at speed 0.75 v_s , and a shock reflected from a density inhomogeneity will hit it with relative velocity $\sqrt{15A_r/16}/(4-A_r)v_s$ (i.e. a Mach number of $\sqrt{3A_r/(4-A_r)}$), where A_r is related to the density contrast, A, by $A = 3A_r (4A_r - 1) / (\sqrt{3A_r (4 - A_r)} - \sqrt{5} (A_r - 1))$ (Sgro 1975). For $A \to \infty$, $A_r = 2.5$ and the maximum Mach number of the reflected shock is $\sqrt{5}$. In order that these secondary shocks propagating back through the shell are supercritical (i.e. that they reflect ions to form a precursor that excites the lower-hybrid waves), they must have Mach number greater than the so-called first critical Mach number. Edmiston & Kennel (1984) in a survey of first critical Mach numbers for various MHD shocks find a value of 1.7 for perpendicular shocks in plasmas with γ (ratio of specific heats) of 5/3 and β (gas pressure/magnetic pressure) of ~ 1. This requires $A_r \simeq 2$ and a density contrast of ~ 30, with lower values required for higher β . For reference the electron density in the shocked x-ray emitting plasma is in the range 10-15 cm^{-3} (Vink, Kaastra, & Bleeker 1996; Favata et al. 1997), while that in the shocked optically emitting knots determined from S II line ratios is $\sim 10^3 - 10^4$ cm⁻³ (Chevalier & Kirshner 1978; Reed et al. 1995). The initial mass density contrast will be increased from the simple ratio of these electron densities since the x-ray emitting plasma is more highly ionized than the optical knots, by a factor of ~ 10 . However the density of the optical knots may also have been enhanced over that due to shock compression by radiative cooling. Chevalier & Kirshner (1978) report densities of $< 100 \text{ cm}^{-3}$ from diffuse (presumably unshocked) S II, which given the difference in ionization state between this and the x-ray emitting plasma still gives sufficient density contrast to reflect supercritical shocks back into the shell.

Whether the ion reflection is diffuse or specular is a harder question to answer. We have assumed a kinetic form for the instability, since this is likely to be more realistic, and also gives a simpler derivation of an analytic form for the electron distribution function. In order to get sufficient time for wave growth to occur ahead of the shock, we are limited to waves with parallel components of wavevector $k_{\parallel}/k = \omega_{pi}/\omega_{pe}$ or greater, in order to have group velocities away from the shock comparable to the shock velocity itself. Specularly reflected ions give rise to much faster growing instabilities, where waves with smaller k_{\parallel} may grow to significant intensities before being overrun by the shock to allow harder electron spectra to be produced, and might conceivably produce a better match to the BeppoSAX MECS/PDS data. This issue of specular versus diffuse ion reflection and the reality of the electron distribution function discussed here is likely to remain an open question at least until high resolution X-ray spectra become available. We note that the electron distribution function produced by the wave activity should have discernable effects on the line spectrum. Ionization and excitation rates will be altered by the extra population of high energy electrons, and modeling of the X-ray spectrum might be the best way to confirm or refute the existence of such an electron distribution function (see Gabriel et al. 1991, for an example). Such an effort is beyond the scope of this paper, and requires high spectral resolution observations where individual lines can observed.

5. Conclusions

We have presented a model based on plasma wave excitation by collisionless shocks to generate a non-thermal electron distribution, the bremsstrahlung from which can explain the hard X-ray "tail" in the spectrum of Cas A, for very reasonable model parameters. This is important because the alternative interpretation, that of X-ray synchrotron emission from cosmic ray electrons with energies of order 10^{14} eV, appears to have been accepted largely on the basis that it is the only interpretation available, though some further observational support for this view is accumulating (Vink et al. 1999; Hwang, Holt, & Petre 2000). Our model is based on observation of the relevant waves and energized electrons at Halley's comet, and analytical and numerical treatments of the process confirming the consistency of the observed electron distribution with the observed wave activity. We have assumed that the wave excitation is associated with shocks which propagate throughout the shell of Cas A, with the waves mainly being generated in ionizing regions of the ejecta, although other mechanisms could be viable. For instance, Begelman & Chiueh (1988) discuss similar waves excited by relative electron-ion drifts in Advection Dominated Accretion Flows. It is also worthwhile to point out that electron acceleration by electrostatic waves is essentially instantaneous on the timescales relevant to supernova remnant evolution, whereas for example stochastic mechanisms (i.e. second order Fermi acceleration) are not (c.f. Blasi 2000).

Similar explanations may also be valid for the supernova remnants RCW 86 and IC 443, for which hard X-ray tails have also been observed. Chevalier (1999) has also expressed scepticism that such emission in IC 443 is due to shock accelerated cosmic ray synchrotron emission. Our discussion has concentrated on Cas A simply because of its well known age, distance, shock velocities, and conspicuous high energy continuum. If proved correct, then this explanation could provide the clearest evidence to date for equipartition of magnetic and thermal energy densities, and the precise shape of the non-thermal bremsstrahlung spectrum should be rich in diagnostic potential for inferring magnetic fields, shock structure and the likely nature of preshock ion driven instabilities.

Finally we note that our non-thermal bremsstrahlung model is qualitatively different to those of previous authors (Asvarov et al. 1990; Sturner, Dermer, & Mattox 1996). Both references consider non-thermal bremsstrahlung in X-rays from the same electron population that produces synchrotron radiation emission, and find that for the hard X-ray tail to be explained in this way, it is likely that too much radio emission would result. Baring, Jones, & Ellison (2000) give a fuller discussion of such scenarios. Our model here postulates a separate electron population which is non-relativistic; basically just a small distortion of the thermal distribution, which need not necessarily be associated with the cosmic ray electron distribution, and so no great change in radio emission should result. This work has been supported by basic research funds of the Office of Naval Research, and has also made use of data obtained from the High Energy Astrophysics Science Archive Research Center (HEASARC), provided by NASA's Goddard Space Flight Center. I am grateful to John Raymond for bringing the comet work to my attention, and to Jacco Vink and Matthew Baring for helpful discussions.

A. Appendix: Lower Hybrid Waves

A.1. Dispersion Relation and Reactive Growth Rate

For cold magnetized electrons the dielectric tensor is

$$K_{ij} = \begin{pmatrix} 1 - \frac{\omega_{pe}^2}{\omega^2 - \Omega_e^2} & i\frac{\Omega_e}{\omega} \frac{\omega_{pe}^2}{\omega^2 - \Omega_e^2} & 0\\ -i\frac{\Omega_e}{\omega} \frac{\omega_{pe}^2}{\omega^2 - \Omega_e^2} & 1 - \frac{\omega_{pe}^2}{\omega^2 - \Omega_e^2} & 0\\ 0 & 0 & \frac{1 - \omega_{pe}^2}{\omega^2} \end{pmatrix}$$
(A1)

where ω_{pe} and Ω_e are the electron plasma and gyrofrequencies respectively. For longitudinal waves we put \mathbf{E} || \mathbf{k} in the wave equation, take the scalar product with \mathbf{k} with the magnetic field along the z-axis and set the result equal to zero to derive the dispersion relation;

$$k_i K_{ij} k_j = (\sin \theta, 0, \cos \theta) K_{ij} \begin{pmatrix} \sin \theta \\ 0 \\ \cos \theta \end{pmatrix} = 0$$
(A2)

which gives

$$K^{L} = 1 - \left(\frac{\omega_{pe}^{2}}{\omega^{2} - \Omega_{e}^{2}}\right) \sin^{2}\theta - \frac{\omega_{pe}^{2}}{\omega^{2}} \cos^{2}\theta = 0.$$
(A3)

To this we can add a term for thermal non-magnetized ions $(1 - \phi(\omega/\sqrt{2}kv_i))\omega_{pi}^2/k^2v_i^2$ where $\phi(x)$ is the usual plasma dispersion function and $v_i = \sqrt{k_B T_i/m_i}$, the ion thermal velocity. In the limit $\omega >> kv_i, \phi(x) \rightarrow 1 + 1/2x^2 + \ldots$ and the well known form for the dielectric tensor for lower hybrid waves results

$$K^{L} = 1 + \frac{\omega_{pe}^{2}}{\Omega_{e}^{2}} \sin^{2}\theta - \frac{\omega_{pi}^{2}}{\omega^{2}} - \frac{\omega_{pe}^{2}}{\omega^{2}} \cos^{2}\theta = 0$$
(A4)

where ω_{pi} is the ion plasma frequency. This yields the dispersion relation $\omega \simeq \omega_{pe}^2$ as $\cos \theta \to 1$ and $\omega \simeq \Omega_{LH}^2$ as $\sin \theta \to 1$. Ω_{LH} is known as the Lower Hybrid frequency and is equal to $\sqrt{\Omega_e \Omega_i}$, with Ω_i being the ion gyrofrequency. We now consider a further ion population moving with velocity U with respect to the stationary plasma. The dispersion relation becomes

$$K^{L} = 1 + \frac{\omega_{pe}^{2}}{\Omega_{e}^{2}} \sin^{2}\theta - \frac{\omega_{pi}^{2}}{\omega^{2}} - \frac{\omega_{pe}^{2}}{\omega^{2}} \cos^{2}\theta - \frac{\omega_{pi}^{\prime 2}}{(\omega - kU)^{2}} = 0.$$
(A5)

For $\cos \theta \to 1$ equation (A5) takes the same form of that for the Buneman instability where Langmuir waves are generated by the ion beam (c.f. Sturrock 1994, pp 113). For $\cos \theta \to 0$ a quartic equation similar to that for the Buneman instability results, but with the replacements $\omega_{pe} \rightarrow \Omega_{LH}$ and $\omega_{pi} \rightarrow \Omega_{LH} \omega'_{pi} / \omega_{pi}$, giving a growth rate

$$\gamma = \frac{\sqrt{3}}{2^{4/3}} \Omega_{LH} \left(\frac{n_i'}{n_i}\right)^{1/3}.$$
 (A6)

Moving away from $\cos \theta = 0$, we put $\omega = \Omega_{LH}$ in the parallel electron term and the ion term to get

$$(\omega - kU)^{2} = \frac{\omega_{pi}^{2\,\prime}}{1 + \frac{\omega_{pe}^{2}}{\Omega_{e}^{2}}\sin^{2}\theta - \frac{\omega_{pe}^{2}}{\Omega_{LH}^{2}}\cos^{2}\theta - \frac{\omega_{pi}^{2}}{\Omega_{LH}^{2}}}.$$
 (A7)

With $kU \sim \Omega_{LH}$ and $\omega_{pe} \gg \Omega_e$, the growth rate γ is

$$\omega - \Omega_{LH} \simeq \pm i\gamma \simeq \pm i \left(\frac{n_i'}{n_i}\right)^{1/2} \frac{\Omega_i}{\cos\theta}.$$
 (A8)

Hence for $\cos\theta \sim \omega_{pi}/\omega_{pe}$, the growth rate is of order Ω_{LH} , falling off as $\Omega_i/\cos\theta$ for larger $\cos\theta$.

As discussed by Begelman & Chiueh (1988) an electromagnetic correction is required in the parallel electron term of K^L . Since waves propagate within $\pm \omega_{pi}/\omega_{pe}$ of the perpendicular direction to the magnetic field, the wave phase speed parallel to the magnetic field can be very large, approaching or exceeding the speed of light. This correction can be written $\omega_{pe}^2 \rightarrow \omega_{pe}^2/(1 + \omega_{pe}^2/k^2c^2)$ (Begelman & Chiueh 1988; Melrose 1986, p 28). We also retain further terms in the expansion; $1/(\omega^2 - \Omega_e^2) \simeq -1/\Omega_e^2(1 + \omega^2/\Omega_e^2 + ...)$, with the last term in parentheses $\simeq \Omega_{LH}^2/\Omega_e^2 \simeq \omega_{pe}^2/k_a^2c^2 \sim \omega_{pe}^2/k^2c^2 \cdot v_{\perp}^2/v_e^2$. Here $v_{\perp}^2 = v_{Ai}^2 + v_e^2$ is the electron velocity perpendicular to the magnetic field, with v_{Ai} the Alfvén velocity, v_e the electron thermal velocity, and c the speed of light. Taking $k \sim \Omega_e/v_{\perp}$, with k_{\parallel} and k_{\perp} being wavevectors parallel and perpendicular to the magnetic field, applying these two corrections yields (see e.g. Vaisberg et al. 1983; McClements et al. 1997)

$$K^{L} = 1 + \frac{\omega_{pe}^{2}}{\Omega_{e}^{2}} \frac{k_{\perp}^{2}}{k^{2}} \left(1 + \frac{\omega_{pe}^{2}}{k_{\perp}^{2}c^{2}} \frac{1}{1 + v_{e}^{2}/v_{Ai}^{2}} \right) - \frac{\omega_{pi}^{2}}{\omega^{2}} - \frac{\omega_{pe}^{2}}{\omega^{2}} \frac{k_{\parallel}^{2}}{k^{2}} \left(1 + \omega_{pe}^{2}/k^{2}c^{2} \right)^{-1}.$$
 (A9)

McClements et al. (1997) discuss reactive growth rates derived using similar dispersion relations for various reflected ion distributions.

A.2. Kinetic Growth Rate and Accelerated Electron Distribution

In the presence of suprathermal electrons and ions, two extra terms are added to the expression for K^L ,

$$+\frac{\omega_{pe}^{\prime 2}}{n_{e}^{\prime}k^{2}}\int\frac{\vec{k}\cdot\vec{v_{e}}}{\omega}\frac{\vec{k}}{\omega-\vec{k}\cdot\vec{v_{e}}}\cdot\frac{\partial f_{e}^{\prime}}{\partial\vec{v_{e}}}d^{3}\vec{v_{e}}+\frac{\omega_{pi}^{\prime 2}}{n_{i}^{\prime}k^{2}}\int\frac{\vec{k}\cdot\vec{v_{i}}}{\omega}\frac{\vec{k}}{\omega-\vec{k}\cdot\vec{v_{i}}}\cdot\frac{\partial f_{i}^{\prime}}{\partial\vec{v_{i}}}d^{3}\vec{v_{i}},\tag{A10}$$

where the primes denote quantities with respect to the suprathermal particle distributions, n'_e and n'_i being the suprathermal electron and ion densities, respectively. The overall growth rate for lower-hybrid waves is found by setting $\omega \to \Omega_{LH} + i\gamma$ and taking the imaginary parts, using the Landau prescription for the terms in equation (A10). This produces a growth rate γ ;

$$2\gamma = \frac{\pi \Omega_{LH}^{3} \omega'_{pi}^{2}}{k^{2} n'_{i}} \left[\omega_{pi}^{2} + \omega_{pe}^{2} \frac{k_{||}^{2}}{k_{\perp}^{2}} \left(1 + \frac{\omega_{pe}^{2}}{k_{\perp}^{2}} \right)^{-1} \right]^{-1} \\ \times \left\{ \int \vec{k} \cdot \frac{\partial f'_{i}}{\partial \vec{v_{i}}} \delta^{3} \left(\Omega_{LH} - \vec{k} \cdot \vec{v_{i}} \right) d^{3} \vec{v_{i}} + \frac{\omega_{pe}^{2}}{\omega_{pi}^{2}} \left(1 + \omega_{pe}^{2} / k^{2} c^{2-1} \right) \frac{\partial f'_{e}}{\partial v_{||}} |_{v_{||} = \Omega_{LH} / k_{||}} \right\}.$$
(A11)

The first term gives wave growth/damping by the suprathermal ions and the second denotes that by suprathermal electrons moving along magnetic field lines. The growth rate due to a Maxwellian ion distribution with temperature T moving with bulk velocity \vec{U} may be evaluated (dropping the term in ω^2/Ω_e^2 in the perpendicular electron term);

$$\gamma_{i} = \frac{\pi}{2} \Omega_{LH}^{3} \frac{n_{i}'}{n_{i}} \left(1 + \frac{\omega_{pe}^{2}}{\omega_{pi}^{2}} \cos^{2} \theta \right)^{-1} \frac{1}{k^{2}} \int \vec{k} \cdot \left(\vec{v_{i}} - \vec{U} \right) \frac{m_{i}}{k_{B}T} \frac{f_{i}'}{n_{i}'} \delta \left(\Omega_{LH} - \vec{k} \cdot \vec{v_{i}} \right) d^{3} \vec{v_{i}} \\ = \frac{1}{2} \sqrt{\frac{\pi}{2}} \frac{n_{i}'}{n_{i}} \left(\frac{\Omega_{LH}}{k\sqrt{k_{B}T/m_{i}}} \right)^{3} \left(1 + \frac{\omega_{pe}^{2}}{\omega_{pi}^{2}} \cos^{2} \theta \right)^{-1} \left(\vec{k} \cdot \vec{U} - \Omega_{LH} \right) \exp \left(\frac{-(\Omega_{LH} - \vec{k} \cdot \vec{U})^{2}}{(2k_{B}T/m_{i})k^{2}} \right).$$
(A12)

The growth rate is maximized for $\left(\vec{k} \cdot \vec{U} - \Omega_{LH}\right) = k\sqrt{k_B T/m_i}$, hence

$$\gamma_{i,max} = \frac{1}{2}\sqrt{\frac{\pi}{2}} \exp\left(-\frac{1}{2}\right) \frac{n_i'}{n_i} \frac{\Omega_{LH}}{\left(1 + \frac{\omega_{pe}^2}{\omega_{pi}^2}\cos^2\theta\right)} \left(\frac{\Omega_{LH}}{k\sqrt{k_BT/m_i}}\right)^2,\tag{A13}$$

which gives strongest wave growth at the smallest possible wavevector, $k_{min} = \omega_{pi}/\sqrt{k_B T/m_i}$. Hence

$$\gamma_{i,max} = 0.38 \frac{\Omega_e^2}{\omega_{pe}^2} \frac{n_i'}{n_i} \frac{\Omega_{LH}}{\left(1 + \frac{\omega_{pe}^2}{\omega_{pi}^2} \cos^2\theta\right)},\tag{A14}$$

and can be seen to be largest for $\cos \theta < \omega_{pi}/\omega_{pe}$, in qualitative agreement with the reactive growth rate. However the kinetic growth rate is smaller by a factor $\sim \Omega_e^2/\omega_{pe}^2$. If the reflected ions have a larger temperature T' than the ambient ion temperature T, the growth rate is smaller still by a factor $\sim T/T'$. Returning to equation(A11) the accelerated electron distribution function is given (with the assumption of steady state conditions, i.e. $\gamma = 0$) by

$$\frac{\omega_{pe}^2}{\omega_{pi}^2} \left(1 + \omega_{pe}^2 / k^2 c^2\right)^{-1} \frac{\partial f'_e}{\partial v_{||}} |_{v_{||} = \Omega_{LH} / k_{||}} = -\frac{n'_i}{\sqrt{2\pi}} \frac{m_i}{k_B T} \exp\left(-\frac{1}{2}\right).$$
(A15)

With some manipulation $\omega_{pe}^2/k^2c^2 = \Omega_{LH}^2/k^2v_{Ai}^2 = \Omega_{LH}^2\cos^2\theta/k_{\parallel}^2v_{Ai}^2 = v_{\parallel}^2\cos^2\theta/v_{Ai}^2$, allowing us to integrate to get f_e ;

$$f'_{e}(v_{||}) = \frac{n'_{i}}{\sqrt{2\pi}k_{B}T/m_{i}} \exp\left(-\frac{1}{2}\right) \frac{\omega_{pi}^{2}}{\omega_{pe}^{2}} \left(v_{m} - v_{||} + \frac{\left(v_{m}^{3} - v_{||}^{3}\right)\cos^{2}\theta}{3v_{Ai}^{2}}\right)$$
(A16)

where $v_{Ae} = v_{Ai}\sqrt{m_i n_i/m_e n_e}$ is the electron Alfvén velocity, v_m is a constant of integration, the maximum velocity where $f(v_m) = 0$, and θ is the angle between the magnetic field direction and the wavevector where the growth rate is a maximum. We may integrate over f'_e in the range $-v_m \rightarrow +v_m$ to obtain an expression for the number density of energized electrons, n'_e . The result is

$$n'_{e} = \frac{n'_{i}}{\sqrt{2\pi}k_{B}T/m_{i}} \exp\left(-\frac{1}{2}\right) \frac{\omega_{pi}^{2}}{\omega_{pe}^{2}} \left(v_{m}^{2} + \frac{v_{m}^{4}\cos^{2}\theta}{2v_{Ai}^{2}}\right).$$
 (A17)

Vaisberg et al. (1983) appear to make the approximation $(1 + \omega_{pe}^2/k^2c^2)^{-1} \simeq 1 - \omega_{pe}^2/k^2c^2$ to derive a slightly different form for the accelerated electron distribution, where v_{Ae} becomes a firm upper limit to $v_{||}$.

A.3. Group Velocity

From equation (A4) with $\omega_{pe} >> \Omega_e$

$$\omega = \frac{\Omega_e}{\omega_{pe}k_\perp} \sqrt{\omega_{pi}^2 \left(k_\perp^2 + k_{||}^2\right) + \omega_{pe}^2 k_{||}^2}.$$
(A18)

Hence the wave group velocity away from the shock front is

$$v_g = \left| \frac{\partial \omega}{\partial k_\perp} \right| = \frac{\omega}{k_\perp} \left[\frac{\omega_{pe}^2 k_{||}^2 + \omega_{pi}^2 k_{||}^2}{\omega_{pi}^2 \left(k_\perp^2 + k_{||}^2 \right) + \omega_{pe}^2 k_{||}^2} \right].$$
(A19)

If $\omega/k_{\perp} \sim U \sim 2v_s$ then $v_g \geq v_s$ for $k_{\parallel}/k_{\perp} \sim \cos\theta \sim \omega_{pi}/\omega_{pe}$. Waves excited with lower $\cos\theta$ have lower group velocities. Since the reflected ions only move a distance downstream on the order of a gyroradius, growth rates need to be several times Ω_i if significant wave growth for these waves is to occur before they are overrun by the shock. Waves at $\cos\theta \sim \omega_{pi}/\omega_{pe}$ and above can stay ahead of the shock and can hence grow to large intensities, even if the growth rate is small. Hence in equation (A17) we simply put $\cos\theta = \omega_{pi}/\omega_{pe}$ and proceed with the calculations of the bremsstrahlung continuum. Similar conclusions result from the use of the dispersion relation with electromagnetic and thermal corrections (McClements et al. 1997), and will be discussed in more detail in future work.

A.4. Applicability Criteria and Connection to Electron Acoustic Waves

Equation (A16) for the accelerated electron distribution assumes waves are generated at a pitch angle to the magnetic field direction given by $\cos \theta = \omega_{pi}/\omega_{pe}$ only, yielding a maximum electron velocity of v_{Ae} . In realistic conditions both the reactive and kinetic instabilities will excite waves with pitch angles down to $\cos \theta = 0$. Consequently waves with phase speeds along the magnetic field, $\Omega_{LH}/k_{||}$, up to c will exist, allowing some electrons to be accelerated up to relativistic energies. However a break in the electron spectrum should still exist at the electron Alfvén speed, v_{Ae} .

In the lower hybrid wave the damping of the ion oscillation by electron screening is inhibited since the electrons are magnetized. This suggests a criterion for the existence of lower hybrid waves of electron gyroradius << wavelength, or $v_e/\Omega_e << v_i/\omega_{pi}$. This can be reexpressed as $T_e << \frac{m_e}{m_i} T_i \Omega_e^2 / \omega_{pi}^2$. Assuming $T_i = \frac{3}{32} m_i v_s^2 / k_B$ for a 4000 km s⁻¹ shock in Cas A (assuming equipartition between ions and magnetic field) gives $T_e \ll 3 \times 10^6$ K. On these grounds we might expect lower hybrid wave acceleration to have ceases in Cas A, since the electrons have been heated by collisional processes to $T_e \sim 4 \times 10^7 \text{K}$. On the other hand this criterion appears not to be met for the plasma conditions near the nucleus of comet Halley, where lower hybrid waves and their associated electron distribution function were in fact observed in situ in 1986 (Gringauz et al. 1986; Klimov et al. 1986), suggesting possibly that it is somewhat naive. From the condition that the electron Landau damping rate be $<< \Omega_{LH}$ we derive $k_B T_e << m_e \Omega_{LH}^2 / k_{\parallel}^2$, which is equivalent to the first inequality if $k_{\parallel}/k = \cos\theta = \omega_{pi}/\omega_{pe}$, but extends to higher electron temperatures for $\cos\theta \to 0$, which would be more consistent with observations. Shapiro et al. (1999), motivated in part by the discovery of cometary x-ray emission, (c.f. Bingham et al. 1997) have recently demonstrated by particle-in-cell simulations that the observed wave activity at comet Halley is indeed consistent with the observed electron distribution function.

If in equation (A4) we put $\phi(x) \to 2x^2 - 4x^4/3 + \dots$ appropriate for hot ions, then with $\Omega_e >> \omega_{pe}$

$$K^{L} = 1 + \frac{1}{k^{2}\lambda_{di}^{2}} - \frac{\omega_{pe}^{2}k_{||}^{2}}{\omega^{2}k^{2}} = 0$$
(A20)

which is equivalent to equation (3.11) of Begelman & Chiueh (1988), their dispersion relation for electron acoustic waves, in the limit of zero ion drift velocity. These authors derived their dispersion relations from fluid equations, assuming the electrons to be strongly magnetized, i.e. $\Omega_e > \omega_{pe}$. This requirement is not necessary here. As discussed by Begelman & Chiueh (1988) these electron acoustic waves have very similar properties to lower hybrid waves. The growth rate for these waves due to a drifting Maxwellian ion distribution may be evaluated in the same way (putting $\omega_{pi} \to 0$ and $\omega'_{pi} \to \omega_{pi}$ in the forgoing) with the result

$$\gamma_{i,max} = \frac{1}{2} \sqrt{\frac{\pi}{2}} \exp\left(-\frac{1}{2}\right) \frac{\omega \omega_{pi}^2}{\omega_{pe}^2 \cos^2 \theta} \left(\frac{\omega}{k\sqrt{k_B T/m_i}}\right)^2.$$
(A21)

REFERENCES

Allen, G. E., et al. 1997, ApJ, 487, L97

Allen, G. E., Petre, R., & Gotthelf, E. V. 1998, AAS, 193, 51.01

Anderson, M. C., & Rudnick, L. 1995, ApJ, 441, 307

- Asvarov, A. I., Dogiel, V. A., Guseinov, O. H., & Kasumov, F. K. 1990, A&A, 229, 196
- Baring, M. G., Jones, F. C., & Ellison, D. C. 2000, ApJ, 528, 776
- Begelman, M. C., & Chiueh, T. 1988, ApJ, 332, 872
- Bingham, R., Dawson, J. M., Shapiro, V. D., Mendis, D. A., & Kellett, B. J. 1997, Science, 275, 49
- Berestetskii, V. B., Lifshitz, E. M., & Pitaevskii, L. P. 1982, Quantum Electrodynamics, (Oxford: Pergamon Press)
- Blasi, P. 2000, ApJ, 532, L9
- Boella, G., et al. 1997, A&AS, 122, 341
- Borkowski, K. J., Blondin, J. M., & Sarazin, C. L. 1992, ApJ, 400, 222
- Borkowski, K. J., Szymkowiak, A. E., Blondin, J. M., & Sarazin, C. L. 1996, ApJ, 466, 866
- Cargill, P. J., & Papadopoulos, K. 1988, ApJ, 329, L29
- Chevalier, R. A., & Kirshner, R. P. 1978, ApJ, 219, 931
- Chevalier, R. A. 1999, ApJ, 511, 798
- Edmiston, J. P., & Kennel, C. F. 1984, J. Plasma Phys., 32, 429
- Favata, F., Vink, J., Dal Fiume, D., Parmar, A. N., Santangelo, A., Mineo, T., Preite-Martinez, A., Kaastra, J. S., & Bleeker, J. A. M. 1997, A&A, 324, L49
- Frontera, F., et al. 1997, A&AS, 122, 357
- Gabriel, A. H., Bely-Dubau, F., Faucher, P., & Acton, L. W. 1991, ApJ, 378, 438
- Gedalin, M. 1996, J. Geophys. Res., 101, 4871
- Gorenstein, P., Kellogg, E. M., & Gursky, H. 1970, ApJ, 160, 199
- Gringauz, K. I., et al. 1986, Nature, 321, 282
- Gull, S. F. 1975, MNRAS, 1975, 171, 263
- Hughes, J. P., Rakowski, C. E., Burrows, D. N., & Slane, P. O. 2000, ApJ, 528, L109
- Hwang, U., Holt, S. S., & Petre, R. 2000, ApJ, 537, in press
- Jun, B.-I., Jones, T. W., & Norman, M. L. 1996, ApJ, 468, L59
- Keohane, J. W., Petre, R., Gotthelf, E. V., Ozaki, M., & Koyama, K. 1997, ApJ, 484, 350

- Keohane, J. W., Gotthelf, E. V., & Petre, R. 1998, ApJ, 503, L175
- Klimov, S. S., et al. 1986, Nature, 321, 292
- Koyama, K., Petre, R., Gotthelf, E. V., Hwang, U., Matsuura, M., Ozaki, M., & Holt, S. S. 1995, Nature, 378, 255
- Koyama, K., Kinugasa, K., Matsuzaki, K., Nishiuchi, M., Sugizaki, M., Torii, K., Yamauchi, S., & Aschenbach, B. 1997, PASJ, 49, L7
- Krasnosel'skikh, V. V., Kruchina, E. N., Thejappa, G., & Volokitin, A. S. 1985, A&A, 149, 323
- Laming, J. M., Raymond, J. C., McLaughlin, B. M., & Blair, W. P. 1996, ApJ, 472, 267
- Laming, J. M. 1998, ApJ, 499, 309
- Lengyel-Frey, D., Thejappa, G., MacDowall, R. J., Stone, R. G., & Phillips, J. L. 1997, J. Geophys. Res., 102, 2611
- Levinson, A. 1996, MNRAS, 278, 1018
- Longair, M. S. 1994, High Energy Astrophysics, Vol. 2, Stars, the Galaxy and the Interstellar Medium (Cambridge: Cambridge University Press)
- McClements, K. G., Dendy, R. O., Bingham, R., Kirk, J. G., & Drury, L. O'C. 1997, MNRAS, 291, 241
- Melrose, D. B. 1986, Instabilities in Space and Laboratory Plasmas, (Cambridge: Cambridge University Press)
- Mochizuki, Y., Takahashi, K., Janka, H.-Th., Hillebrandt, W., & Diehl, R. 1999, A&A, 346, 831
- Reed, J. E., Hester, J. J., Fabian, A. C., & Winkler, P. F. 1995, ApJ, 440, 706
- Sgro, A. G. 1975, ApJ, 197, 621
- Shapiro, V. D., Bingham, R., Dawson, J. M., Dobe, Z., Kellett, B. J., & Mendis, D. A. 1999, J. Geophys. Res., 104, 2537
- Slane, P., Gaensler, B. M., Dame, T. M., Hughes, J. P., Plucinsky, P. P., & Green, A. 1999, ApJ, 525, 357
- Sturner, S. J., Dermer, C. D., & Mattox, J. R. 1996, A&AS, 120, 445
- Sturrock, P. A. 1994, Plasma Physics, (Cambridge: Cambridge University Press)
- Sutherland, R. S. 1998, MNRAS, 300, 321
- Tanimori, T., et al. 1998, ApJ, 497, L25

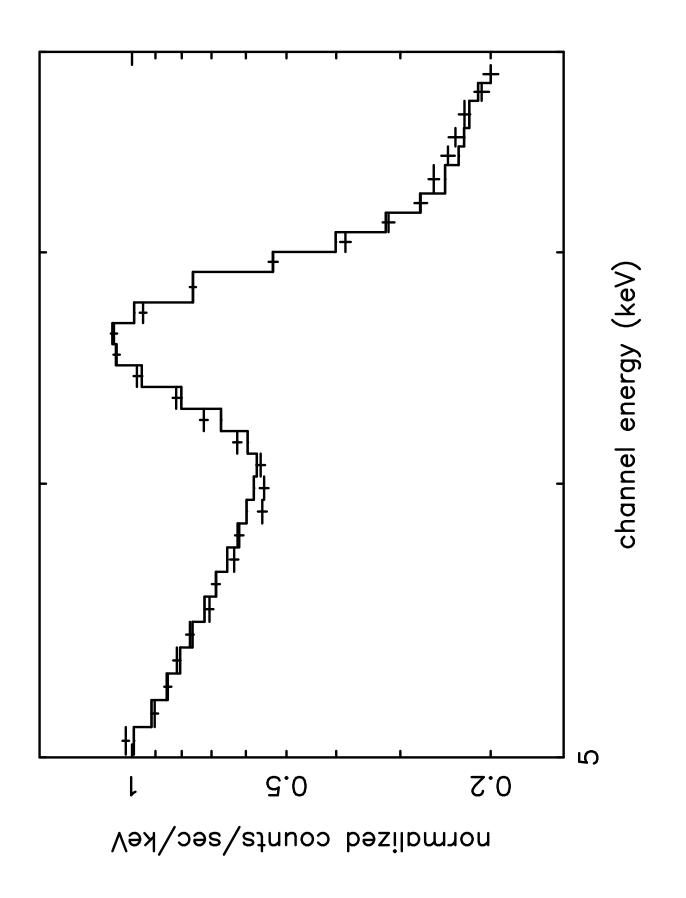
- The, L.-S., Leising, M. D., Kurfess, J. D., Johnson, W. N., Hartmann, D. H., Gehrels, N., Grove, J. E., & Purcell, W. R. 1996, A&AS, 120, 357
- Tokar, R. L., Aldrich, C. H., Forslund, D. W., & Quest, K. B. 1986, Phys. Rev. Lett., 56, 1059
- Vaisberg, D. L., Galeev, A. A., Zastenker, G. N., Klimov, S. I., Nozdrachev, M. N., Sagdeev, R. Z., Sokolov, A. Y., & Shapiro, V. D. 1983, Sov. Phys. JETP, 58, 716
- Vink, J., Kaastra, J. S., & Bleeker, J. A. M. 1996, A&A, 307, L41
- Vink, J., Bloemen, H., Kaastra, J. S., & Bleeker, J. A. M. 1998, A&A, 339, 201
- Vink, J., Concetta Maccarone, M., Kaastra, J., Mineo, T., Bleeker, J. A. M., Preite-Martinez, A., & Bloemen, H. 1999, A&A, 344, 289
- Vink, J., Kaastra, J. S., Bleeker, J. A. M., & Bloemen, H. 2000, AdSpR, 25, 689
- Woods, L. C. 1987, Principles of Magnetoplasma Dynamics, (Oxford: Oxford University Press)

This preprint was prepared with the AAS IAT_EX macros v5.0.

Fig. 1.— Data and fit for the spectral region around the Fe K feature at 6.7 keV taken from the BeppoSAX MECS spectrum. The temperature fitted to the thermal bremsstrahlung continuum is 3.3 keV.

Fig. 2.— Data from the BeppoSAX MECS and PDS instruments, with model bremsstrahlung spectra for a fully ionized pure oxygen plasma. The softest model is pure thermal bremsstrahlung at 3.3 keV temperature. The harder spectra come from electron distribution functions appropriate to lower hybrid wave energization, for electron Alfvén velocities of 32, 40, and 48 atomic units. The fraction of electrons in the non-thermal distribution is 4%.

Fig. 3.— Same data as for figure 2, but with model spectra for pure thermal and nonthermal bremsstrahlung corresponding to an electron Alfvén velocities of 56, 68, and 80 atomic units, for fully ionized helium.



laming 11-Jan-2000 14:32

